Ion-Binding Study by ^{17}O Solid-State NMR Spectroscopy in the Model Peptide Gly-Gly-Gly at 19.6 T

Eduard Y. Chekmenev,*,† Kevin W. Waddell,‡,§ Jun Hu,†,‖ Zhehong Gan,†
Richard J. Wittebort,‡ and Timothy A. Cross*,†,‖,#

*Contribution from the NMR Program, National High Magnetic Field Laboratory (NHMFL),
Tallahassee, Florida 32310, Department of Chemistry, University of Louisville,
Louisville, Kentucky 40292, Vanderbilt Institute of Imaging Science, Vanderbilt University,
Nashville, Tennessee 37232, Department of Chemistry & Biochemistry, Florida State University,
Tallahassee, Florida 32306, and Institute of Molecular Biophysics, Florida State University,
Tallahassee, Florida 32306*

Received March 9, 2006; E-mail: eduard_chekmenev@hotmail.com (E.Y.C.); cross@magnet.fsu.edu (T.A.C.)

Abstract: Li$^+$ and Ca^{2+} binding to the carbonyl oxygen sites of a model peptide system has been studied by ^{17}O solid-state NMR spectroscopy. ^{17}O chemical shift (CS) and quadrupole coupling (QC) tensors are determined in four Gly-(Gly-^{17}O)-Gly polymorphs by a combination of stationary and fast magic-angle spinning (MAS) methods at high magnetic field, 19.6 T. In the crystal lattice, the carbonyl oxygen of the central glycyl residue in two gly-gly-gly polymorphs form intermolecular hydrogen bonds with amides, whereas the corresponding carbonyl oxygens of the other two polymorphs form interactions with Li$^+$ and Ca^{2+} ions. This permits a comparison of perturbations on ^{17}O NMR properties by ion binding and intermolecular hydrogen bonding. High quality spectra are augmented by density functional theory (DFT) calculations on large molecular clusters to gain additional theoretical insights and to aid in the spectral simulations. Ion binding significantly decreases the two ^{17}O chemical shift tensor components in the peptide plane, δ_{11} and δ_{22}, and, thus, a substantial change in the isotropic chemical shift. In addition, quadrupole coupling constants are decreased by up to 1 MHz. The effects of ion binding are found to be almost an order of magnitude greater than those induced by hydrogen bonding.

Introduction

Oxygen sites are responsible for a great deal of chemistry catalyzed by biological macromolecules. Carbonyl groups are of special interest because they directly participate in interactions that (i) define protein 2° and 3° structure, (ii) play a crucial role in intermolecular contacts, and (iii) are direct participants in numerous biological functions. Here, we exploit NMR at high magnetic fields to study ion binding to peptide carbonyl oxygens. Such cation−oxygen interactions play a key role in the selectivity filters of ion channels and, thus, are critical for ion transport across membranes.[1,2] The measurement of perturbations in ^{17}O NMR properties induced by interactions with cations potentially allows for an assessment of a variety of biologically important structural and functional information. We find that ^{17}O NMR of carbonyl oxygens interacting with cations is a highly sensitive probe for structure, function, and dynamics in proteins.

Oxygen NMR spectroscopy has not been extensively used due to a number of intrinsic problems. It is a spin $^5/_2$ nucleus with a large quadrupole coupling, ~6 MHz, has low natural abundance, 0.037%, and a low gyromagnetic ratio, 1/7 that of ^{1}H. Together, these pose significant experimental difficulties associated with a poor signal-to-noise ratio (S/N) and large spectral widths. Nevertheless, recent advances in the development of high-field magnets and NMR instrumentation have substantially improved S/N and spectral resolution,[3] resulting in the rapid growth of ^{17}O NMR spectroscopy in the past few years.[4−6]

Significant effort has been applied toward the study of hydrogen bonding by ^{17}O NMR spectroscopy in a number of small model systems,[7−9] where the values and the orientations of the chemical shift (CS) and quadrupole coupling (QC) tensor components can be obtained in polycrystalline powders or in single crystals. In combination with X-ray diffraction structures, detailed interpretation of the tensor parameters is possible.

† National High Magnetic Field Laboratory.
‡ University of Louisville.
§ Vanderbilt University.
‖ Department of Chemistry & Biochemistry, Florida State University.
Institute of Molecular Biophysics, Florida State University.

(1) Doyle, D. A.; Cabral, J. M.; Pfuetzner, R. A.; Kuo, A. L.; Gulbis, J. M.; Cohen, S. L.; Chait, B. T.; MacKinnon, R. *Science* **1998**, *280*, 69−77.
(2) MacKinnon, R. *FEBS Lett.* **2003**, *555*, 62−65.
(3) Gan, Z. H.; Gor'kov, P.; Cross, T. A.; Samoson, A.; Massiot, D. *J. Am. Chem. Soc.* **2002**, *124*, 5634−5635.
(4) Lemaitre, V.; Smith, M. E.; Watts, A. *Solid State Nucl. Magn. Reson.* **2004**, *26*, 215−235.
(5) Wu, G. *Biochem. Cell Biol.* **1998**, *76*, 429−442.
(6) Zhu, X. H.; Zhang, N. Y.; Zhang, Y.; Zhang, X. L.; Ugurbil, K.; Chen, W. *NMR Biomed.* **2005**, *18*, 83−103.
(7) Takahashi, A.; Kuroki, S.; Ando, I.; Ozaki, T.; Shoji, A. *J. Mol. Struct.* **1998**, *442*, 195−199.
(8) Wu, G.; Yamada, K.; Dong, S.; Grondey, H. *J. Am. Chem. Soc.* **2000**, *122*, 4215−4216.
(9) Zhang, Q. W.; Chekmenev, E. Y.; Wittebort, R. J. *J. Am. Chem. Soc.* **2003**, *125*, 9140−9146.
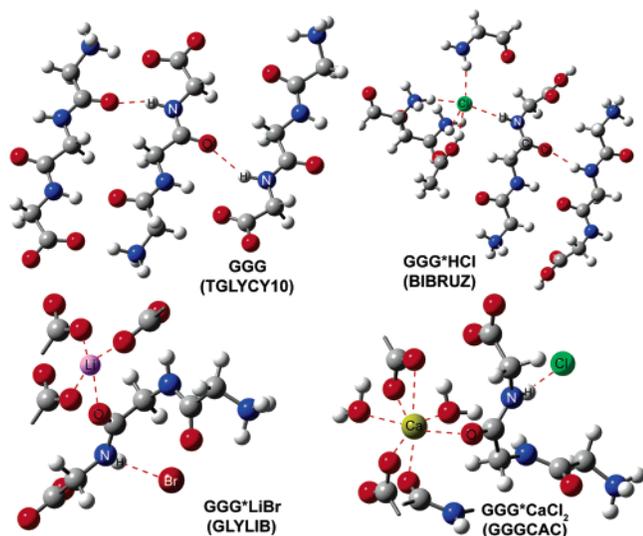
Figure 1. X-ray structures of four triglycine polymorphs.[12-15] The central carbonyl amide group of each gly-gly-gly interacts with neighboring gly-gly-gly molecules through hydrogen bonding in GGG and GGG*HCl or with cations (Li^{+} and Ca^{2+}) in GGG*LiBr and GGG*CaCl₂. The central amide N—H interacts by intermolecular hydrogen bonding with a neighboring O=C in GGG, with Cl^{−} in GGG*HCl and GGG*CaCl₂, and with Br^{−} in GGG*LiBr. Peptide torsion angles of the central residue correspond to an extended conformation in GGG, GGG*HCl, and GGG*LiBr and to an α-helix in GGG*CaCl₂. Atom color codes are: red − oxygen, blue − nitrogen, gray − carbon, green − chloride, white − hydrogen, pink − lithium, brown − bromide, and yellow − calcium. Abbreviations in parentheses correspond to Cambridge Structural Database (CSD) codes.

However, ion binding, important for protein catalytic and ion conductance activities, has not been investigated in detail by ^{17}O NMR spectroscopy.

Although protein ^{17}O NMR studies were recently suggested as being feasible and attractive as a result of sensitivity to the local perturbations,[4,5] there are very few reports investigating carbonyl sites in peptides and proteins.[10,11] Moreover, there is little experimental information about site specific carbonyl oxygen interactions with the exception of a few hydrogen bonding studies in small model systems and poly-amino acids. Here we present a systematic examination of [17]O chemical shifts and quadrupole couplings in crystalline polymorphs of the model tripeptide gly-gly-gly. This tripeptide is studied here in four different conformations.[12-15] Two polymorphs form antiparallel β-sheets and their central carbonyl groups form C=O···H−N intermolecular hydrogen bonding with O···H distances of 2.18 and 2.00 Å, correspondingly (Figure 1). The central carbonyl of a third antiparallel β-sheet polymorph interacts with a Li^{+} ion at a distance of 1.95 Å, whereas the carbonyl oxygen of a right-handed α-helix polymorph binds Ca^{2+} at a distance of 2.30 Å. This series provides a unique opportunity to study ion binding by solid-state NMR spectroscopy in a relatively small peptide system. Additionally, the effects of adjacent residues are eliminated, because all four polymorphs have the identical

peptide sequence. Consequently, it is possible to model ion binding interactions occurring in proteins in a significantly simplified, but relevant, model system. Density functional theory (DFT) calculations are used to investigate the effects of ion binding and hydrogen bonding on carbonyl ^{17}O NMR parameters theoretically. The effects of the former are shown to be an order of magnitude greater than the latter demonstrating the excellent potential for ^{17}O NMR to study gating and selectivity in ion channels.[1,16]

Methods

Sample Preparation. Fmoc-[17]O-Gly was prepared by exchange of glycine, 400 mg, with 70% H₂[17]O, 500 mg, (Cambridge Isotope Laboratories, Inc., Andover, MA) at 100 °C under acidic conditions, HCl(g), pH < 1.[17] Gly-([17]O-Gly)-Gly was prepared by Fmoc solid-phase peptide synthesis from ~50% enriched Fmoc-[17]O-Gly, purified by ion exchange chromatography, and crystallized in four different conformations, GGG*HCl,[13] GGG,[15] GGG*LiBr,[12] and GGG*CaCl₂,[14] as described previously.[18,19]

Solid-State NMR Spectroscopy. Solid-state NMR spectroscopy was performed on instruments with Bruker data acquisition systems at 14.1 and 19.6 T. Spectrometers were equipped with a Bruker triple-resonance MAS probe (14.1 T) or an in-house double-resonance MAS probe (19.6 T).[20] All spectra were referenced externally to the [17]O chemical shift of liquid H₂O. The MAS experiments utilized a rotor synchronized spin−echo sequence with an echo delay of 50 μs. Pulse (180°) widths were 3.5−4.0 μs, and spinning rates were ~20 kHz (19.6 T) and 12 kHz (14.1 T). The static experiments used a 10 μs echo delay. The repetition rate ranged from 1.5 to 3 s with a ¹H B₁ (decoupling) field of 70 kHz.

DFT Calculations. [17]O electric-field gradient (EFG) and chemical-shift tensors were calculated for isolated tripeptide molecules and clusters of molecules using the Gaussian98 program[21] in the University of Kentucky Computing Center and in the Advanced Biomedical Computing Center, NCI−Frederick. The DFT tensor computations employ the B3LYP functional and the Dunning correlation consistent double-ζ basis set (aug-cc-pVDZ),[22] which contains both diffuse and polarization functions. Because the aug-cc-pVDZ basis set was not available for Br^{−}, Cl^{−}, and Ca^{2+}, the ions utilized the 6-311++g(d,p) basis set instead of the aug-cc-pVDZ basis set. EFG tensor components in atomic units, q_{ij}, are related to the quadrupole coupling tensor components, χ_{ij}, by $\chi_{ij} = 6.01\ q_{ij}$ MHz[9,23] utilizing the accepted value of the nuclear quadrupole moment Q = −2.558.[24] CS components, δ_{ij}, are reported relative to water using the absolute [17]O shielding scale, $\delta_{ij} = 307.9 - \sigma_{ij}$.[25]

Calculations in Monomers. The tripeptide monomers were constructed based on the X-ray coordinates for heavy atoms (non-hydrogens) and hydrogen positions were optimized by the Pople type 6−31 g* basis set prior to the calculations of the NMR parameters.

Calculations in Clusters. Clusters were constructed based on X-ray diffraction coordinates, and hydrogen positions were optimized by the Pople type 6−31 g* basis set. In cases of ion-containing clusters,

(10) Hu, J.; Chekmenev, E. Y.; Gan, Z. H.; Gor'kov, P. L.; Saha, S.; Brey, W. W.; Cross, T. A. *J. Am. Chem. Soc.* **2005**, *127*, 11922−11923.
(11) Lemaitre, V.; de Planque, M. R. R.; Howes, A. P.; Smith, M. E.; Dupree, R.; Watts, A. *J. Am. Chem. Soc.* **2004**, *126*, 15320−15321.
(12) Meuleman, R.; Piret, P.; Vanmeers, M. *Acta Crystallogr., Sect. B: Struct. Sci.* **1971**, *27*, 1187−1190.
(13) Lalitha, V.; Subramanian, E. *Cryst. Struct. Commun.* **1982**, *11*, 561−564.
(14) Van der Helm, D.; Willoughby, T. V. *Acta Crystallogr., Sect. B: Struct. Sci.* **1969**, *B25*, 2317−2326.
(15) Srikrishnan, T.; Winiewicz, N.; Parthasarathy, R. *Int. J. Pept. Protein Res.* **1982**, *19*, 103−113.

(16) Tian, F.; Cross, T. A. *J. Mol. Biol.* **1999**, *285*, 1993−2003.
(17) Steinschneider, A.; Burgar, M. I.; Buku, A.; Fiat, D. *Int. J. Pept. Protein Res.* **1981**, *18*, 324−333.
(18) Chekmenev, E. Y.; Xu, R. Z.; Mashuta, M. S.; Wittebort, R. J. *J. Am. Chem. Soc.* **2002**, *124*, 11894−11899.
(19) Chekmenev, E. Y.; Zhang, Q. W.; Waddell, K. W.; Mashuta, M. S.; Wittebort, R. J. *J. Am. Chem. Soc.* **2004**, *126*, 379−384.
(20) Solid State NMR Facilities at NHMFL. http://nmr.magnet.fsu.edu/facilities/solids.htm.
(21) Frisch, M. J.; et al. *Gaussian 98*, revision A.7; Gaussian, Inc.: Pittsburgh, PA, 1998.
(22) Woon, D. E.; Dunning, T. H. *J. Chem. Phys.* **1993**, *98*, 1358−1371.
(23) Yamada, K.; Dong, S.; Wu, G. *J. Am. Chem. Soc.* **2000**, *122*, 11602−11609.
(24) Pyykko, P. *Z. Naturfors. Sect. A: J. Phys. Sci.* **1992**, *47*, 189−196.
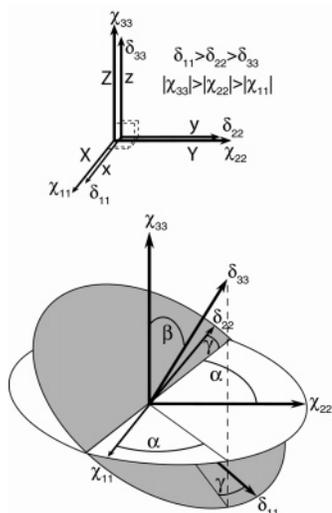(25) Wasylishen, R. E.; Mooibroek, S.; Macdonald, J. B. *J. Chem. Phys.* **1984**, *81*, 1057−1059.

Figure 2. Reference frames of the CS and QC tensors and the Euler angles (α, β, γ), which relate the orthogonal systems of the CS and QC tensors. The transition from QC to CS principal axis system is achieved by a series of three 2D rotations: (i) α rotates the CS system about the Z axis (χ_{33}), (ii) β is a rotation about the newly formed y axis (the intercept of the two planes), and (iii) γ is a rotation about the z axis (δ_{33}). [27]
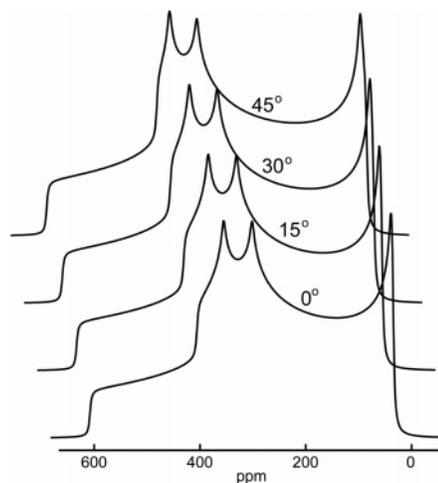

Figure 3. Simulated superimposed [17]O static spectral array with a variation in α, the most insensitive Euler angle. Parameters used in the simulations: $\delta_{11} = 533$ ppm, $\delta_{22} = 420$ ppm, $\delta_{33} = -36$ ppm, $\chi = 8.2$ MHz. $\eta = 0.28$.

GGG*CaCl$_2$ and GGG*LiBr, where DFT calculations failed due to convergence problems, the hydrogen positions were optimized at the restricted Hartee−Fock (RHF) level of theory with the same basis set. The coordinates used for calculations are provided in the Supporting Information. DFT tensor calculations were performed after geometry optimization in all cases. The GGG cluster consisting of 72 atoms includes the central gly-gly-gly molecule and two hydrogen-bonded gly-gly-gly molecules, as shown in Figure 1. The GGG*HCl cluster (89 atoms) incorporates the central gly-gly-gly molecule, one more gly-gly-gly molecule H-bonded to the central carbonyl, and the Cl$^-$ ion interacting with the H−N of the central glycyl residue. Note that Cl$^-$ is chelated by four molecular fragments of the neighboring gly-gly-gly molecules, Figure 1. The GGG*LiBr cluster (152 atoms) and GGG*CaCl$_2$ cluster (191 atoms) include the central triglycine molecule interacting with Li$^+$ via $\cdots$O=C and Br$^-$ via $\cdots$H−N for GGG*LiBr, Ca^{2+} via $\cdots$O=C, and Cl$^-$ via $\cdots$H−N for GGG*CaCl$_2$ augmented by a relatively large part of the crystal lattice. Note that only the core of the cluster is shown in Figure 1 for GGG*CaCl$_2$ and GGG*LiBr. The implementation of a rather large cluster serves two purposes: (i) it helps with hydrogen geometry optimization and (ii) the charge distributions are better modeled near the site of interest.[26] Because GGG*CaCl$_2$ and GGG*LiBr clusters are large, only the central molecule and ions used the computationally demanding basis set, whereas the rest of the atoms utilized the 3-21 g* basis.

Data Simulation and Error Assessment. Both static and MAS ^{1}H decoupled [17]O spectra were simulated by an in-house-developed Matlab program and independently by the WSOLIDS1 program,[27] providing identical fits. Solid state ^{17}O NMR spectral fits are inherently difficult because eight independent parameters contribute to the line shapes and the procedure used here is similar to that described previously by Wu and co-workers.[23] These include three principal components of the CS tensor, quadrupole coupling and asymmetry, and three Euler angles, α, β, γ, describing the mutual orientation of the CS and QC tensor principal axis frames. The choice of the Euler angles aligns δ_{33} along the z axis, δ_{22} along the y axis, δ_{11} along the x axis, χ_{zz} along the Z axis, χ_{yy} along the Y axis, and χ_{zz} along the X axis in the (x, y, z) and (X, Y, Z) reference frames, Figure 2.[23,27] A noteworthy feature of

multidimensional simulations is the multiple combinations of (α, β, γ) producing identical theoretical line shapes. To alleviate this degeneracy, we use an initial estimate based on our DFT calculations along with the single-crystal solid-state NMR data from central glycyl carbonyls in similar peptides.[28] This allows us to start searching the multidimensional space of the NMR parameters in close proximity to the correct NMR parameter set. In the next step, the MAS spectrum is simulated to validate the initial estimate for δ_{iso} and the two independent parameters $(\chi$ and $\eta)$ of the traceless QC tensor. This is possible because high-speed, high-field MAS line shapes are relatively insensitive to variations in the CS principal components and the relative orientation of the CS and QC tensors. The other five parameters, three Euler angles and two CS principal components, are obtained by fitting the static spectrum. Because powder patterns, in particular the very wide spectra observed here, are subject to substantial intensity distortions, the five experimentally well-defined shoulder or peak positions were emphasized in the fits.[29] The β Euler angle is within $1-2°$ of $90°$ and, as a result, the spectral fits are relatively insensitive to variations in α, Figure 3. This greatly simplifies the fitting procedure by reducing the number of variables to three: the angle γ and two components of the CS tensor. In this way, the procedure uses 8 experimental numbers (3 and 5, respectively, from the MAS and powder spectra) to determine the 8 NMR parameters. The simulations were then iteratively repeated again for MAS and static spectra to satisfy a single set of fitted parameters. With $\beta \approx 90°$, simulations corresponding to (γ) and $(180-\gamma)$ are nearly indistinguishable. DFT calculations and results from single-crystal studies were employed for selecting the correct parameter. Uniqueness and approximate uncertainties of these parameters were established by a Monte Carlo search of the parameter space for the powder spectra. To make this practical, the 8-dimensional parameter space was reduced by fixing α at the fitted value, fixing the isotropic shift at the MAS value, and searching the remaining parameters with 10^6 Monte Carlo steps over ranges in the neighborhood of the fitted parameters: ± 0.5 MHz for χ, ± 0.4 for η, ± 10 ppm for CS principal components, $\pm 3°$ for β, and $\pm 10°$ for γ. Parameter values yielding calculated spectra in which any of the 5 characteristic powder pattern frequencies differed from experiment by more than $4-5$ ppm were discarded, and the reported uncertainties (Table 1) are the standard deviations of the accepted parameter sets. Within these ranges, the fits are unique, and we note that the two QC parameters, χ and η, were highly correlated.

(26) Waddell, K. W.; Chekmenev, E. Y.; Wittebort, R. J. *J. Am. Chem. Soc.* **2005**, *127*, 9030−9035.
(27) Eichele, K.; Wasylishen, R. E. *WSOLID1 NMR Simulation Package*, 1.17.30; 2001.
(28) Waddell, K. W.; Chekmenev, E. Y.; Wittebort, R. J. *J. Phys. Chem. B* **2006**, in press.
(29) Oas, T. G.; Drobny, G. P.; Dahlquist, F. W. *J. Magn. Reson.* **1988**, *78*, 408−424.

Table 1. Experimental and Calculated DFT CS and QC Tensors[a]

system	χ	η	δ_{11}	δ_{22}	δ_{33}	δ_{span}[b]	δ_{dev}[c]	δ_{iso}[d]	α[e]	β	γ
GGG*CaCl$_2$(exp)	7.4(0.28)	0.70(0.14)	427(4)	337(3)	−24(3)	451(5)	361(4)	247(3)	0°(10)	90°(2)	116°(3)
monomer	8.54	0.18	603	450	−47	650	497	335	27°	93°	77°
cluster	7.66	0.49	432	352	−18	450	371	255	4°	89°	106°
GGG*LiBr(exp)	7.5(0.5)	0.32(0.22)	453(10)	365(8)	−43(10)	496(14)	408(13)	258(8)	10°(10)	87°(2)	72°(6)
monomer	8.63	0.42	564	423	−44	608	467	314	17°	92°	75°
cluster	8.14	0.57	473	373	−39	512	412	269	12°	83°	70°
GGG*HCl(exp)	7.9(0.24)	0.48(0.10)	535(5)	395(4)	−52(4)	587(6)	447(6)	293(4)	0°(10)	90°(2)	105°(2)
monomer	8.58	0.22	621	444	−71	692	515	331	8°	91°	106°
cluster	8.66	0.31	576	420	−43	619	463	318	8°	92°	92°
GGG(exp)	8.20(0.20)	0.28(0.07)	533(4)	420(3)	−50(4)	583(5)	470(5)	301(3)	0°(10)	90°(2)	80°(2)
monomer	7.95	0.32	555	377	−58	613	435	291	4°	89°	107°
trimer	8.61	0.28	560	394	−36	595	430	306	2°	90°	75°

[a] CS components are in ppm with respect to external liquid water and quadrupole couplings, $\chi = \chi_{33}$, are in MHz. Euler angles specify the relative orientations of the CS and QC tensors as illustrated in Figure 2.[23,33] Estimated uncertainties in experimental parameters (see Methods) are in parentheses. [b] $\delta_{span} = (\delta_{11} - \delta_{33})$ [c] $\delta_{dev} = (\delta_{22} - \delta_{33})$ [d] $\delta_{iso} = (\delta_{11} + \delta_{22} + \delta_{33})/3$. [e] Note, when $\alpha \approx 0°$, simulations with γ or $180° - \gamma$ are indistinguishable and the value listed conforms to that observed in single-crystal studies.
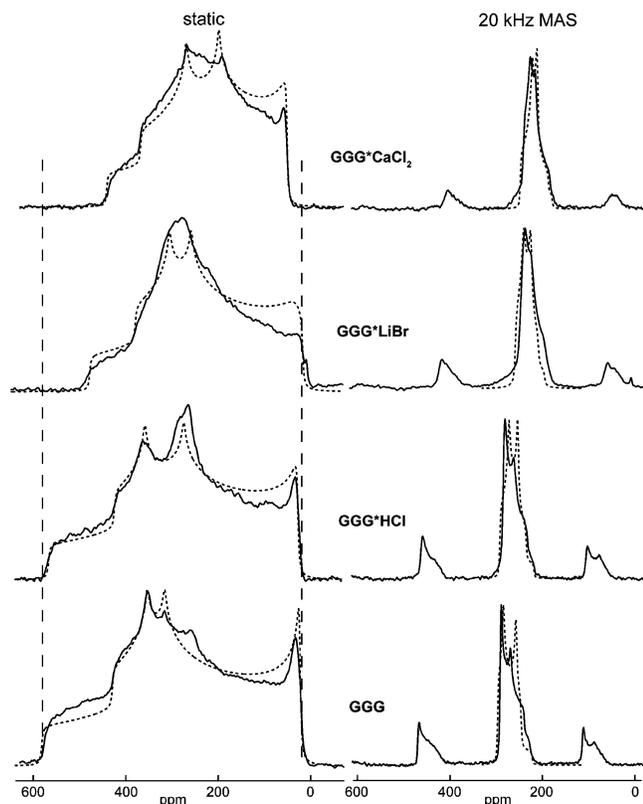

Figure 4. Static and 20 kHz MAS ^{17}O ^{1}H-decoupled spectra (solid) and simulations (dashed) of Gly-(^{17}O-Gly)-Gly crystallized in four different conformations acquired at 19.6 T. The spectra were obtained from 8−12 mg samples and ∼10−16k and ∼64k transients for MAS and static experiments, respectively.

For example, calculated spectra are approximately unchanged if χ is decreased by 0.2 MHz and η is increased by 0.1.

Results and Discussion

NMR Results. The stationary and MAS spectra with high S/N recorded at 19.6 T are shown in Figure 4. The four sets of spectra for various gly-gly-gly polymorphs exhibit significant ^{17}O line shape sensitivity for intermolecular interactions. The 19.6 T spectra were simulated (dashed line, Figure 4), and the fit quality was tested for the GGG polymorph at 14.1 T by exploiting the quadrupole line-shape dependence on B_0. Both MAS and static spectra obtained at 14.1 T were well simulated (Figure 5) using the parameters obtained at 19.6 T without
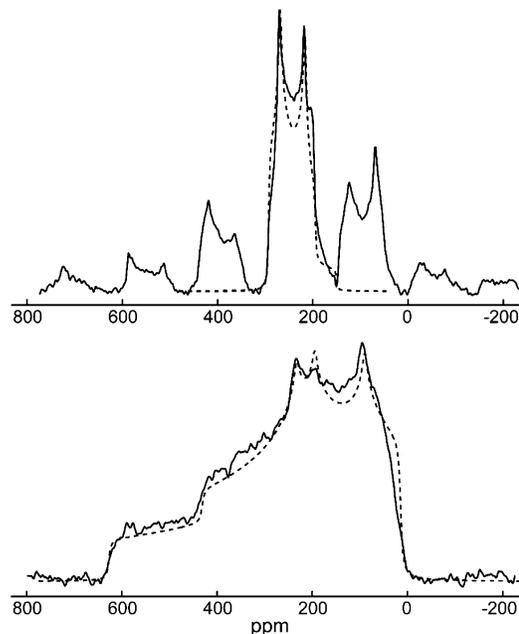

Figure 5. Static and 12 kHz MAS ^{17}O ^{1}H-decoupled spectra (solid) and simulations (dashed) of Gly-(^{17}O-Gly)-Gly crystallized in the GGG conformation, acquired at 14.1 T. The simulations use the results obtained at 19.6 T: $\delta_{11} = 533$ ppm, $\delta_{22} = 420$ ppm, $\delta_{33} = -50$ ppm, $\chi = 8.2$ MHz. $\eta = 0.28$, $\alpha = 0°$, $\beta = 90°$, $\gamma = 80°$. ^{17}O-enriched peptide (45 mg) was used to obtain static and MAS spectra with 9400 and 22 600 transients, respectively.

modification, thereby validating the 19.6 T spectral analysis.

The ^{17}O NMR parameters obtained from MAS and stationary spectral fits are summarized in Table 1. Additionally, the range of CS and QC principal component values and their relative orientations are illustrated in Figure 6. Both CS and QC parameters found in GGG and GGG*HCl polymorphs, i.e., without cations in the lattice, are very similar to those obtained previously for poly-alanine,[7,30] poly-glycine,[31,32] and the WAL*P*23 peptide in a lipid environment.[11] Moreover, the GGG polymorph with hydrogen-bonding contacts, C=O···H−N−C=^{17}O···H−N (Figure 1), yielded quadrupole coupling, χ and η, and chemical shielding parameters, δ_{11}, δ_{22}, and δ_{33}, that agree well with site-

(30) Yamauchi, K.; Kuroki, S.; Ando, I.; Ozaki, T.; Shoji, A. *Chem. Phys. Lett.* **1999**, *302*, 331−336.
(31) Kuroki, S.; Takahashi, A.; Ando, I.; Shoji, A.; Ozaki, T. *J. Mol. Struct.* **1994**, *323*, 197−208.
(32) Yamauchi, K.; Kuroki, S.; Ando, I. *J. Mol. Struct.* **2002**, *602*, 171−175.
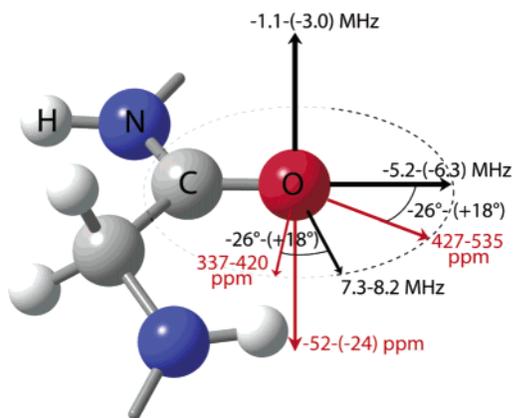
Figure 6. Experimental CS and QC principal component orientations of the central carbonyl oxygen in four gly-gly-gly peptides in the molecular frame based on the canonical orientation of the QC tensor in amides.[23] δ_{11}, δ_{22}, χ_{33}, and χ_{22} lie in the peptide plane, whereas δ_{33} and χ_{11} are perpendicular to the peptide plane.

specific values obtained for central glycyl carbonyls in ala-gly-gly and gly-gly-val tripeptides.[28] The GGG*HCl polymorph with Cl⁻···H−N−C=^{17}O···H−N intermolecular interactions (Figure 3) demonstrates somewhat similar CS parameters, but rather smaller quadrupole coupling constant and asymmetry, which could be explained by the indirect effect via N−H hydrogen bonding to the negatively charged Cl⁻ ion. This is similar to the indirect hydrogen bonding effects observed in the carboxyl oxygen in oxalic acid.[9]

Variation of Experimental NMR Parameters. Experimentally determined QC and CS principal components and their relative orientations are listed in Table 1 for the four polymorphs. Although CS parameters are more accurately determined than QC parameters (see Methods), differences among the polymorphs are large compared to the estimated uncertainties. A noteworthy result is the range of isotropic shifts. In this set of four peptides, δ_{iso} varies over a range of 54 ppm, which is approximately twice the range of ^{15}N isotropic shifts in proteins. We conclude that ^{17}O NMR parameters are sensitive monitors of conformation and chemical environment.

Comparing the peptides in which the target carbonyl is hydrogen bonded to an amide (GGG or GGG*HCl) to those in which the oxygen is coordinated to a cation (GGG*LiBr or GGG*CaCl₂) shows a significant effect that can be attributed to ion binding. Ion binding decreases χ by ~0.7 MHz, increases η by 0.2, shifts δ_{iso} upfield by ~50 ppm, and decreases the span of the shielding tensor by ~100 ppm. We note that the parameters determined here for hydrogen-bonded carbonyls are in good agreement with those previously reported.[8,9,23,30] For example, carbonyl oxygens of β-sheet polyglycine (χ = 8.3 MHz, η = 0.29, δ_{11} = 562 ppm, δ_{22} = 410 ppm, and δ_{33} = −108 ppm[31]) are in close agreement with those reported here for the sheetlike GGG polymorph (Table 1) in which both CO and NH of the target peptide group are H-bonded.

Unique to the solid-state experiment is the ability to relate tensor data to molecular geometry. Because the powder sample experiments used here determine only the relative orientations of the CS and QC tensors, we augment this with single crystal results and quantum chemical calculations, which indicate that molecular orientations of the QC tensors are (i) not highly variable and (ii) conveniently positioned in the peptide molecular frame.[23,28] The component of smallest magnitude, χ_{11}, is normal

to the peptide plane, and χ_{22} is close to the C=O bond. Consequently, the largest component, χ_{33}, is in the peptide plane and perpendicular to C=O. This and the relative CS tensor orientations based on the Euler angles (Table 1) are summarized in Figure 6. In the four examples studied here, the most shielded (upfield) component, δ_{33}, is close to χ_{11} (the peptide plane normal) and δ_{11} and δ_{22} are rotated relative to χ_{22} and χ_{33} in the peptide plane. The most deshielded component, δ_{11}, is closest to χ_{22} (the C=O bond) with the angle of rotation varying from +18° for GGG*LiBr (toward N of the previous residue) to −26° for GGG*CaCl₂ (toward Cᵅ of the same residue). In this reference frame, the carbonyl oxygen CS components most affected by replacing hydrogen bonds with ions are those in the peptide plane. Both δ_{11} and δ_{22} are shifted upfield, by ~100 and ~60 ppm, respectively, whereas the component perpendicular to the peptide plane, δ_{33}, is less affected and moves downfield by ~20 ppm. Note that Ca²⁺ is nearly in the peptide plane with the O···Ca²⁺ bond vector being 31° from the peptide plane and 31° from the C=O bond vector. Li⁺ orientation in the molecular frame is somewhat different with the O···Li⁺ bond vector being 24° from the peptide plane and 50° from the C=O bond vector.

NMR Parameters from Quantum Chemical Calculations. To quantify the effects of replacing hydrogen bonds with ions at the target peptide NH and CO groups, density functional theory (DFT) calculations were employed. Calculations are reported for "monomers" (all lattice interactions including those with ions stripped away) and clusters (constructed so that these interactions are included). The rmsd between the DFT and experimental CS principal components is 20 ppm for the clusters and 78 ppm for the monomers, indicating that the calculations are sufficiently accurate to model the effects of local intermolecular interactions on NMR parameters. Although QC parameters are somewhat overestimated, this is a typical difficulty for most DFT computational methods.[9] On the basis of prior experience with simpler systems and larger clusters, we anticipate that a significant contribution to theoretical error is cluster incompleteness, i.e., neglect of some local interactions within 4−6 Å.[9,34] For example, in this peptide series, three compounds have strong intermolecular interactions of the peptide plane with ion: GGG*HCl, GGG*LiBr, and GGG*CaCl₂. Among these three, GGG*HCl has the smaller cluster size in our DFT calculations: 89 atoms compared to 152 and 191 atoms, correspondingly. As a consequence, the smallest cluster size of GGG*HCl resulted in a larger theoretical error for isotropic chemical shift: 25 ppm compared to 11 and 8 ppm, correspondingly. Larger clusters were not implemented due to computational demands.

Monomers and Local Geometry. Insofar as the peptides studied here are short and charged, the monomer calculations reflect both local conformation and how this conformation adjusts the local electric field. In particular, the different conformations present the nearby carboxy terminus, which is negatively charged in the three zwitterions (GGG, GGG*LiBr, and GGG*CaCl₂) and uncharged in the cationic GGG*HCl in different ways. The calculations show some variation in quadrupole coupling constants and more significant variations

(33) Power, W. P.; Wasylishen, R. E.; Mooibroek, S.; Pettitt, B. A.; Danchura, W. *J. Phys. Chem.* **1990**, *94*, 591−598.

(34) Strohmeier, M.; Stueber, D.; Grant, D. M. *J. Phys. Chem. A* **2003**, *107*, 7629−7642.

Table 2. Comparison of Direct and Indirect Ion Binding Effects on the NMR Properties Obtained from DFT Calculations of Clusters and Single Molecules

difference[a]	indirect	direct	$\Delta\Delta\chi$	$\Delta\Delta\eta$	$\Delta\Delta\delta_{11}$	$\Delta\Delta\delta_{22}$	$\Delta\Delta\delta_{33}$	$\Delta\Delta\delta_{iso}$
"HCl"−"GGG"	OC→Cl^{-b}	same	−0.58	+0.13	−50	−41	6	−28
"CaCl$_2$"−"HCl"	same	HN→Ca^{2+e}	−0.96	+0.22	−126	−74	1	−66
"CaCl$_2$"−"GGG"	OC→Cl^{-b}	HN→Ca^{2+e}	−1.54	+0.35	−176	−115	7	−95
"LiBr"−"HCl"	Cl$^-$→Br^{-c}	HN→Li^{+f}	−0.57	+0.06	−46	−26	−23	−32
"LiBr"−"GGG"	OC→Br^{-d}	HN→Li^{+f}	−1.1	+0.19	−96	−67	−17	−60

^{a} "GGG", "HCl", "CaCl$_2$", and "LiBr" indicate parameter differences between cluster and monomer calculations for GGG, GGG*HCl, GGG*CaCl$_2$, and GGG*LiBr, respectively. ^{b} N−H hydrogen bond to O=C replaced with the bond to Cl$^-$. ^{c} N−H hydrogen bond to Cl$^-$ replaced with the bond to Br$^-$. ^{d} N−H hydrogen bond to O=C replaced with the bond to Br$^-$. ^{e} C=O hydrogen bond to H−N replaced with the bond to Ca^{2+}. ^{f} C=O hydrogen bond to H−N replaced with the bond to Li$^+$.

in chemical shifts. For example, the two monomers based on GGG and GGG*LiBr are both zwitterionic and have similar local conformations. Consequently, their CS parameters are similar but still differ on average by 23 ppm. Also somewhat similar in shielding parameters are the monomers with the GGG*CaCl$_2$ and GGG*HCl conformations. Because these have different secondary motifs based on the ϕ and ψ torsion angles and different overall charges, an interplay between local conformation and the interaction of the peptide group with charged groups is implied. Because the experimental CS and QC parameters are strongly correlated with the group interacting with the carbonyl oxygen, we anticipate that the latter is dominant.

Clusters and Intermolecular Interactions. To assess the effect of the lattice environment on CS and QC, we compare the differences in the NMR properties between monomer and cluster calculations. In monomers, the intermolecular interactions are missing, whereas they are present in the clusters. These differences in the peptide series permit a decomposition of the effects of various intermolecular interactions on the NMR parameters. In this procedure, we have assumed that the various interactions affecting the NMR parameters are additive, and this is justified by the self-consistency of the results. "Conformation independent", pairwise comparisons between peptides are made by a second subtraction of parameters, which are listed in Table 2. Because the peptides studied here are systematically hydrogen bonded at the direct (CO) and indirect (NH) sites in different ways (see Figure 1), the individual effects upon replacing a hydrogen bond with a counterion can be estimated. The difference of the difference parameters for GGG (direct and indirect hydrogen bonds) and GGG*CaCl$_2$ (hydrogen bonds replaced by Cl$^-$ and Ca^{2+}) gives an estimate of the combined effects, $\Delta\Delta\delta_{iso} = 95$ ppm. Next, comparing in the same way GGG*CaCl$_2$ with GGG*HCl (only the indirect hydrogen bond is replaced with Cl$^-$) provides an estimate of the direct ion binding effect, $\Delta\Delta\delta_{iso} = 66$ ppm. Thus, a somewhat smaller value, ∼29 ppm, is estimated for the replacement at the indirect site. Alternatively, comparing GGG*HCl and GGG gives a consistent value of 28 ppm at the indirect position, which is confirmed by the other QC and CS parameters. Changes in NMR parameters in GGG*LiBr are approximately half that of GGG*CaCl$_2$. This is likely due to the combination of two factors: Li$^+$ is less positively charged compared to Ca^{2+}, and Br$^-$ is a significantly larger ion than Cl$^-$ and is distanced further from the N atom by 0.28 Å. Considering that the indirect ion-binding effect is approximately half that of the direct ion-binding

effect, we qualitatively conclude that divalent ions have a greater influence on the NMR parameters than monovalent ions.

Conclusion

Poor sensitivity, resolution, and complex parameter sets have experimentally impeded the routine use of ^{17}O in biomolecular NMR studies. Here, high-quality spectra (with S/N > 40) were obtained from 40−60 μmol of ^{17}O per site using a 19.6 T field strength. Reported here are the QC and CS tensor characterizations for the central glycyl carboxyl group in a series of tripeptide polymorphs. DFT calculations for CS and QC components and relative tensor orientations are in good agreement with experiment. Combined experimental and theoretical results demonstrate an excellent sensitivity of the ^{17}O QC and CS interactions to ion binding. Moreover, the effect of ion binding is analyzed with respect to hydrogen bonding interactions, which are nearly always present in proteins. Earlier efforts were limited to studies of the impact of hydrogen bonding on ^{17}O CS and QC with respect to single molecules in a vacuum by theoretical calculations.[7,8,23,31] Additionally, the isolated effects from direct and indirect ion interactions have been characterized by the DFT calculations.

On the basis of experimentally validated DFT calculations, we conclude that (i) hydrogen bonding has a very small impact on CS properties, whereas (ii) the indirect ion interactions have a much more significant influence on the CS properties and a substantial impact on the QC properties, and (iii) direct ion interaction effects on the ^{17}O NMR parameters are approximately twice that of the indirect effects. Thus, ^{17}O NMR is a very sensitive tool for the characterization of ion binding.

In biological systems such as ion channels, indirect and direct ion binding may not be simultaneously present, because the secondary elements of the protein are stabilized by hydrogen-bonding interactions. Thus, only one of those interactions may be present. In the ion selectivity filter of KcsA[1] and other K$^+$ channels, as well as in the ion binding site of gramicidin A,[35] the carbonyl oxygens play the dominant role in ion solvation.[1,16,36−39] Therefore, the ion influence on the ^{17}O parameters may be expected to be smaller by approximately one-third compared to those observed in GGG*CaCl$_2$ and GGG*LiBr polymorphs. Nevertheless, these effects are very large and readily observable by ^{17}O NMR spectroscopy.[10]

(35) Busath, D. D. *Annu. Rev. Physiol.* **1993**, *55*, 473−501.
(36) Gulbis, J. M.; Doyle, D. A. *Curr. Opin. Struct. Biol.* **2004**, *14*, 440−446.
(37) Tajkhorshid, E.; Nollert, P.; Jensen, M. O.; Miercke, L. J. W.; O'Connell, J.; Stroud, R. M.; Schulten, K. *Science* **2002**, *296*, 525−530.
(38) Sui, H. X.; Han, B. G.; Lee, J. K.; Walian, P.; Jap, B. K. *Nature* **2001**, *414*, 872−878.
(39) Fu, D. X.; Libson, A.; Miercke, L. J. W.; Weitzman, C.; Nollert, P.; Krucinski, J.; Stroud, R. M. *Science* **2000**, *290*, 481−486.

Supporting Information Available: Tables of coordinates for the monomers and clusters of the four GGG conformations presented here. Complete ref 21. This material is available free of charge via the Internet at http://pubs.acs.org.

JA060191R